



Resistive plate chambers for tomography and radiography

C. Thomay¹, P. Baesso¹, D. Cussans¹, J. Davies¹, P. Glaysher¹, S. Quillin², S. Robertson², C. Steer², C. Vassallo¹, and J. Velthuis¹

¹University of Bristol, Department of Particle Physics H H Wills Physics Laboratory, Tyndall Avenue, BS8 B1TL Bristol, UK

²AWE, Aldermaston, RG7 4PR Reading, UK

Correspondence to: C. Thomay (christian.thomay@bris.ac.uk)

Received: 18 July 2012 – Published in Geosci. Instrum. Method. Data Syst. Discuss.: 31 August 2012

Revised: 29 November 2012 – Accepted: 10 December 2012 – Published: 19 December 2012

Abstract. Resistive plate chambers (RPCs) are widely used in high energy physics for both tracking and triggering purposes, due to their excellent time resolution, rate capability, and good spatial resolution. RPCs can be produced cost-effectively on large scales, are of rugged build, and have excellent detection efficiency for charged particles. Our group has successfully built a muon scattering tomography (MST) prototype, using 12 RPCs to obtain tracking information of muons going through a target volume of $\sim 50\text{ cm} \times 50\text{ cm} \times 70\text{ cm}$, reconstructing both the incoming and outgoing muon tracks. The required spatial granularity is achieved by using 330 readout strips per RPC with 1.5 mm pitch. The RPCs have shown an efficiency above 99% and an estimated intrinsic resolution below 1.1 mm. Due to these qualities, RPCs serve as excellent candidates for usage in volcano radiography.

1 Introduction

Resistive plate chambers (RPCs) are currently widely used in high energy physics and astrophysics. Since their introduction in the early 1980s (Santonico and Cardarelli, 1981), they have undergone a constant evolution that led to several families of detectors, each of them characterized by specific features in terms of performance, operational mode and geometric setup of the detectors themselves (Fonte, 2002). Nevertheless, all such families share the same principle of operation (Riegler and Lippmann, 2004) and favourable characteristics, which contribute to the rapid diffusion and acceptance of RPCs within the scientific community: low cost per unit area, high rate capability, ruggedness, high detection ef-

iciency for minimum ionizing particles and excellent time resolution.

Typically RPCs are used to provide trigger and timing signatures while the spatial information they obtain is complemented by more accurate detectors. However, it has been shown that a spatial resolution better than 1 mm (Jin et al., 2008) can be achieved with specifically designed RPCs. This result suggests that RPCs could be used in a series of applications where the requirements on the particle interaction position are not too strict. An example of such an application is muon scattering tomography (MST), in which cosmic muons are tracked before and after they penetrate a target volume (see Fig. 1).

By studying the distribution of the scattering angles, it is possible to create a density map of the materials contained in the volume and probe for the presence of high Z materials, such as special nuclear materials.

The idea of using MST for homeland security has already proven feasible and appealing (Schultz et al., 2007); several studies are evaluating the use of RPCs for such applications (Cox et al., 2008). We are working with the Atomic Weapons Establishment (AWE) to develop a prototype MST system and evaluate its performance.

The purpose of this work is to detail the performance of RPCs in our area of application, then to give an account of the applicability of RPCs to problems in geological radiography.

2 Setup

The basic detector unit in our prototype is a 2-mm float glass RPC: two sheets of glass measuring $58\text{ cm} \times 58\text{ cm}$ are glued to a 4-cm-wide glass frame, so that the gas gap has a volume of $50\text{ cm} \times 50\text{ cm} \times 2\text{ mm}$. The gas mixture used to perform

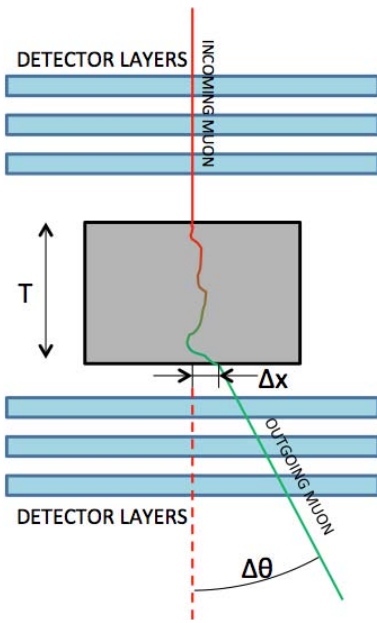


Fig. 1. Muon scattering tomography principle. The muon passes through the upper detectors, scatters in the target, and leaves via the lower detectors. The measured scatter angle allows for estimation of the target Z .

the tests described in this work is composed of Ar (60 %), freon gas R134A (30 %) and C_4H_{10} (10 %).

The external surfaces of the detector are spray painted with Charleswater Statguard to obtain a surface resistivity of $10^5 \Omega/\square$. On top of each RPC sits a printed circuit board which hosts the pickup strips. In the current setup each board hosts 330 strips with 1.5 mm pitch. Once all the dead areas on the detector are taken into account, the actual sensitive area remaining measures approximately $50 \text{ cm} \times 50 \text{ cm}$.

The signal induced on the strips is fed to a hybrid board supporting four HELIX chips. The HELIX (ZEUS collaboration, 2007) is a family of $0.8\text{-}\mu\text{m}$ CMOS readout chips originally designed for the HERA-B experiment and optimized for silicon microstrip detectors and gaseous chambers. Each chip features 128 analog inputs with programmable shaper and amplifiers and a single analog output. When a trigger is received, the analog values at the inputs are sampled and multiplexed onto the output. Currently the trigger is provided by two $50 \text{ cm} \times 50 \text{ cm}$ scintillators placed at the top and bottom of the prototype. An external analog to digital converter is then used to digitize the data; for this we use the commercial CAEN V1724, which also provides clock signals to all the electronics, thus assuring the synchronous operation of the system. Since each hybrid board hosts a daisy chain of 4 HELIX chips, the 330 analog samples from a single RPC can be digitized using a single channel of the V1724.

Our system is comprised of 12 RPCs, hosted in six aluminium cassettes to provide XY readout. The cassettes slide into a cabinet that provides mechanical support and allows



Fig. 2. Picture of the fully assembled system. The six aluminium cassettes contain two RPCs each and provide XY readout. The cassettes also provide connections for high voltage, low voltage, data and gas lines. The gas mixing system is visible at the bottom of the cabinet.

the spacing between detectors to be adjusted; the system is shown in Fig. 2: it is currently set to allow a central gap of $\sim 70 \text{ cm}$, within which a standard sized suitcase could be inserted.

3 Results

The digitized samples from the RPCs are analysed by removing the pedestal and applying a Gaussian fit algorithm, which provides the hit position for the muon on each layer. The noise consists of two components: random noise and correlated noise. The latter is known as common mode. While the random noise is simply Gaussian and results in a random contribution to the signal, one can correct for common mode noise by exploiting that the offset in the signal of the hit strips is correlated to the offset in the strips that were not hit. This requires particular care: as a consequence of the way in which the strips are routed to the HELIX and the grounding scheme adopted on the front-end boards, the common mode presents some discontinuities that could potentially produce erroneous hit reconstructions (see Fig. 3). However, this issue and the presence of noisy strips are both taken into account in the hit finding algorithms. The signal-to-noise ratio for the signals on different layers ranges from 25 to 90: the variation is mainly due to variations in the RPC module noise.

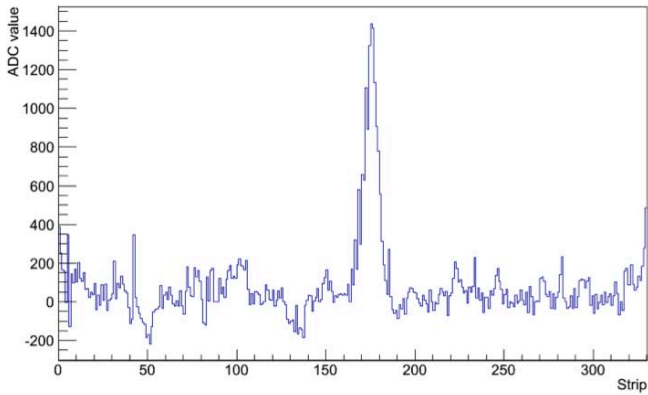


Fig. 3. Signal induced on the strips once the pedestal has been removed. The y-axis shows the converted digital value of the charge deposited in each strip; 1000 ADC counts correspond to ca. 50 pC. The peak due to a muon is clearly visible around strip 175.

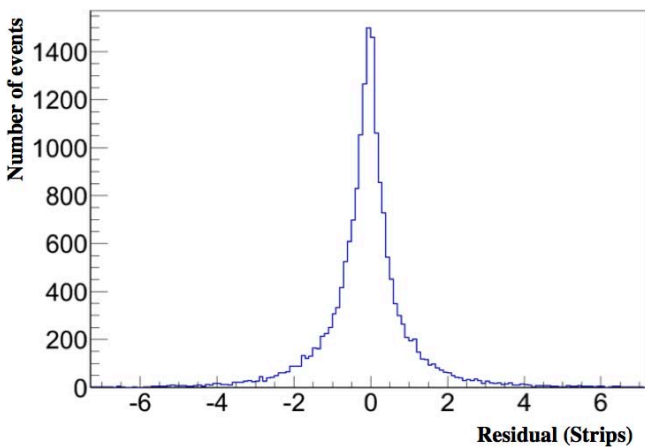


Fig. 4. Distribution of the residuals ($X_{\text{estimated}} - X_{\text{hit}}$) for one of the layers. The x-axis is measured in 1.5-mm strips.

Once the hit position on each layer has been determined, the algorithm attempts to fit a straight line across the six layers. A cut on the χ^2 value ensures that the track is actually due to a single particle and that there are no false hits or multiple hits. Even with this simple approach, we managed to achieve a detection efficiency above 99 % and a purity (defined as the ratio between hits corresponding to muon tracks and all hits including noise) better than 95 %.

To test the spatial resolution of the detectors, we removed one of them from the linear fit and proceeded to estimate the residual distribution (Glaysher, 2012). The result for one layer is shown in Fig. 4.

It is important to note that this corresponds to the raw resolution (σ_{raw}), i.e. including the error due to multiple scattering within the detector and the error due to the extrapolation of the track. A MC simulation study was performed (Vassallo, 2012) in order to estimate the intrinsic resolution σ_{intr} (i.e. the distance between the actual muon position and the

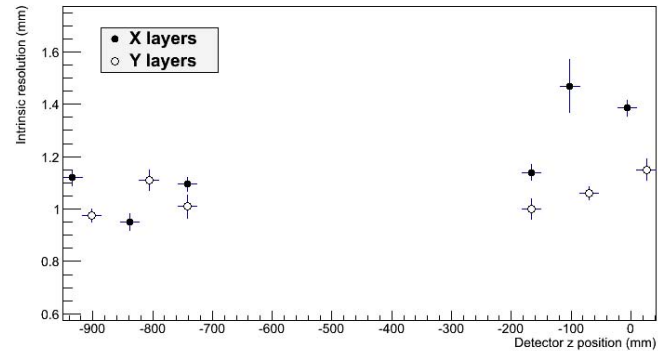


Fig. 5. Intrinsic detector resolution σ_{intr} in mm vs. detector position.

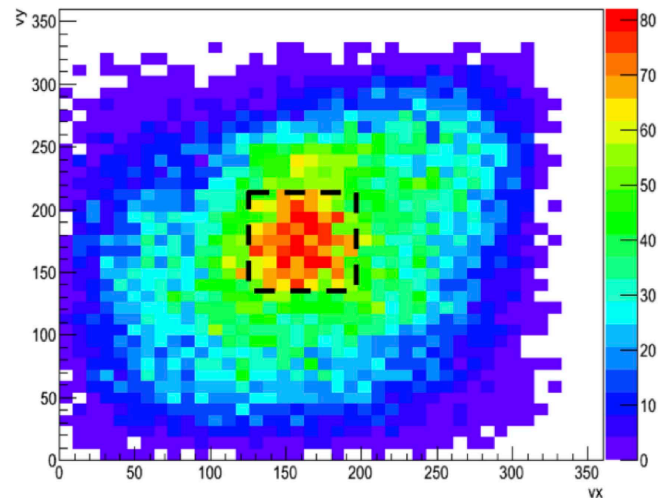


Fig. 6. Reconstructed vertex positions for events with a scattering angle larger than 30 mrad due to the presence of a lead block of $10 \times 15 \times 10 \text{ cm}^3$. Units along the x- and y-axis represent the strip number; each strip is 1.5 mm wide. The “true” position of the lead block is outlined.

reconstructed hit) that would lead to the raw resolution we observed; this resulted in an estimate of $\sigma_{\text{intr}} \approx 1.1 \text{ mm}$ (see Fig. 5). We expect a larger value for the outer layers, since those hits are less strongly constrained by the straight line fit.

Each muon track is split into its top and bottom components, and a combined algorithm fits tracks and vertex positions; thereby the scattering angle can be calculated. The detector volume is then divided into voxels and filled according to the number of tracks that scatter within it. Although this is a very simple approach and does not make full use of tomography techniques, it is nevertheless sufficient to prove the correct behaviour of the prototype. To test it, we placed a block of lead sized $10 \text{ cm} \times 10 \text{ cm} \times 15 \text{ cm}$ in the scanner volume and analysed the data obtained. Figure 6 shows a preliminary analysis of ca. 2 hours of data acquisition: the higher scattering angles are concentrated in the area where we placed the block.

4 Application to volcano radiography

Volcano radiography aims to obtain a measure of the density distribution within a geological target by reconstructing cosmic muons tracks that passed through. By comparison to the muon flux from the incidence direction (which can be obtained from simulation or measured on-site), an estimate of the target's density can be derived from the muon flux attenuation. Reconstruction of the muon track requires at least two layers of detectors in the x- and y-plane; the larger the surface area and the acceptance, the less time of data taking is required to acquire sufficient statistics to estimate the target's density profile. In order to reduce background, it is advantageous to perform time-of-flight measurements, so as to only take into account muons coming from the target direction.

In terms of detector hardware, MST and volcano radiography share many requirements. In volcano radiography, the large distance between detector and target requires good angular resolution; assuming a spatial resolution of 1.1 mm and spacing of 70 cm between the layers, our RPCs could provide an angular resolution of ~ 1.6 mrad and an acceptance of ~ 1.4 sr.

In order to do time-of-flight measurements, good time resolution is needed. RPCs are easily capable of achieving a time resolution on the order of ns. Our current system is not optimised for this, since time-of-flight measurement is not of particular interest in MST. However, we are in the process of upgrading our readout to use the MAROC chip (Blin et al., 2010), which will result in a time resolution better than 10 ns. Furthermore, there are other chips available (in the ROC family of chips developed at LAL-Orsay, for instance) that in combination with our RPCs could achieve time resolution on the order of ns.

Due to the rough environment in which the detectors would be deployed, ruggedness and stability, as well as ease of use, remote readout and low power consumption are all desirable features. RPCs have proven to be very stable, and our system can be read out and controlled via a simple ethernet connection. In terms of power consumption, our current system draws $\sim 2 \text{ W m}^{-2}$, but this is again not optimised for field usage and can be improved accordingly. Finally, while RPCs generally require constant gas flushing, we are currently investigating “sealed-for-life” options where the gas would only have to be changed every few months. Even without this, though, a pre-mixed gas volume could be deployed together with the detector, flushing the gas at intervals automatically.

5 Conclusions and outlook

RPCs are widely adopted by the high energy physics and astrophysics community, but their use outside these very specific fields is still somewhat limited. Both muon scattering tomography and volcano radiography could take advantage

of this technology and of the knowledge developed by its application in experiments across the world.

We have built and tested a muon tracking system based on high resolution RPCs. The system is working as expected, allowing us to correctly track cosmic muons. The preliminary results show that the spatial resolution is better than 1.1 mm, leading to an angular resolution below 1.6 mrad, enough to be successfully used for MST. A simple analysis of the data collected by the detector shows a block of lead placed within the central gap.

We are currently in the process of upgrading our system to use the MAROC chip for readout. This will allow us to utilise the self-triggering capability inherent in our RPCs; the new readout boards also allow for remote ethernet readout. In addition, we are working on the scaling of our system to large areas, as well as investigating “sealed-for-life” options.

In conclusion, we have shown that RPCs are well suited for purposes in volcano radiography: their good spatial/temporal resolution, ruggedness of build, scalability to large sizes, and remote readout all make them excellent candidates for usage in the field.

Edited by: C. Carloganu

References

- Blin, S., Barrillon, P., and de La Taille, C.: MAROC, a generic photomultiplier readout chip, *J. Instrum.*, 5, C12007, doi:10.1109/NSSMIC.2010.5874062, 2010.
- Cox, L., Adsley, P., O'Malley, J., Quillin, S., Steer, C., and Clemett, C.: Detector Requirements for a Cosmic Ray Muon Scattering Tomography System, *Nuclear Science Symposium Conference Record*, 706–710, 2008.
- Fonte, P.: Applications and New Developments in Resistive Plate Chamber, *IEEE T. Nucl. Sci.*, 49, 881–887, 2002.
- Glaysheer, P.: Muon Scattering Tomography, Masters Thesis University of Bristol, 2012.
- Jin, Y., Jianping, C., Qian, Y., Yuanjing, L., Jin, L., Yucheng, W., and Hao, Y.: Studies on RPC position resolution with different surface resistivity of high voltage provider, *Nuclear Science Symposium Conference Record*, 917–918, 2008.
- Riegler, W. and Lippmann, C.: The physics of Resistive Plate Chambers, *Nucl. Instrum. Methods*, 518, 86–90, 2004.
- Santonico, R. and Cardarelli, R.: Development of Resistive Plate Counters, *Nucl. Instrum. Methods*, 187, 377–380, 1981.
- Schultz, L. J., Blanpied, G. S., Borozdinand, K. N., Fraser, A. M., Hengartner, N. W., Klimenko, A. V., Morris, C. L., Oram, C., and Sossong, M. J.: Statistical Reconstruction for Cosmic Ray Muon Tomography, *IEEE T. Image Process.*, 16, 1985–1993, 2007.
- Vassallo, C.: Muon Scattering Tomography, Masters Thesis University of Bristol, 2012.
- ZEUS collaboration: The design and performance of the ZEUS Micro Vertex detector, *Nucl. Instrum. Methods*, 581, 656–686, 2007.